A Novel Narrowband Interference Suppression Method for OFDM Radar

Gor Hakobyan
Robert Bosch GmbH, Corporate Research,
Renningen, 70465 Stuttgart, Germany
Email: Gor.Hakobyan@de.bosch.com

Bin Yang
Institute of Signal Processing and System Theory
University of Stuttgart, Germany
Email: Bin.Yang@iss.uni-stuttgart.de

***Abstract*—The interference between automotive radar sensors becomes a major issue with the increasing number of radars integrated in vehicles for comfort and safety functions. The state-of-the-art radars, typically operating with frequency modulated continuous wave (FMCW) modulation, can be regarded as narrowband interferers for a high bandwidth orthogonal frequency division multiplexing (OFDM) radar with comparably short duration of OFDM symbols. In this paper, we analyze the impact of such interferers on OFDM radar, give a signal model of OFDM radar in presence of interference and discuss the effect of signal processing steps on the latter. Additionally, we present an interference suppression algorithm suitable for any type of narrowband interference. We show in simulations that a considerable interference suppression can be achieved and verify the presented algorithm with measurements.**

***Index Terms*—OFDM radar, interference, linear prediction**

I. Introduction

The number of vehicles equipped with radar sensors is growing constantly. This increases the importance of interference robustness of radars and motivates the research of new radar approaches and interference suppression techniques. A radar with OFDM signal generation has been studied by several research groups [1]–[7], mainly due to the possibility of combining radar functionality with communications [2]–[4]. Due to the flexibility available with digital generation of arbitrary waveforms, OFDM is believed to have a potential for better interference-robustness, achievable with interference-robust waveforms and waveform diversity between OFDM radars [8]. Whereas in [9] the interference-robustness of an OFDM radar in presence of other OFDM radars is studied, the performance of the former in presence of interference from state-of-the-art FMCW radars remains an open issue. To address this issue, in this work we study the interference robustness of the OFDM radar in presence of a state-of-the-art FMCW radar with slow ramps and present an interference suppression algorithm effective against such interferers.

Even though the current FMCW radars can cover a bandwidth as large as the bandwidth of an OFDM radar, their signals can still be considered as a narrowband interference for the latter, since due to the long ramp duration (typically in ms range) only a limited bandwidth is occupied by the FMCW signal within one OFDM symbol (typically in μs range). We analyze the interference robustness of OFDM radar against such interferers and describe the effect of OFDM signal processing steps on the interfering signal. We show that through the OFDM signal processing the interference is decorrelated, i.e. spread in the distance-velocity (d,v) space, and thus is reduced with the integration gain of two-dimensional (2D) fast Fourier transform (FFT). Furthermore, we present an interference suppression method designed against arbitrary narrowband interferences. The proposed interference suppression algorithm is able to achieve a further increase of the signal-to-interference ratio (SIR) via exclusion of the affected subcarriers from evaluation. The signal values of the excluded subcarriers are recovered by a forward-backward linear prediction (FBLP) from the values of neighboring subcarriers. The results show an SIR improvement of 12–$16\,\mathrm{dB}$ depending on the power ratio between desired and interfering signals at the input.

II. OFDM Signal Model and Signal Processing

In the following, an OFDM signal model that serves as a basis for the interference suppression algorithm in Section III is presented. We also describe signal processing steps for distance-velocity estimation and their impact on the interfering signal. Whereas the OFDM radar signal processing steps are generally well known, in this section we point out their influence on the interfering signal.

For distance-velocity estimation, a sequence of OFDM symbols is transmitted and the reflections from the surrounding objects are received. The μ-th transmitted OFDM symbol in baseband can be represented as

$$x_\mu(t) = \frac{1}{N_\mathrm{c}} \sum_{n=0}^{N_\mathrm{c}-1} s_\mu(n) e^{j2\pi n \Delta f (t - T_\mathrm{CP})} \tag{1}$$

where N_c is the number of OFDM subcarriers, $s_\mu(n)$ is the complex modulation symbol transmitted on the n-th subcarrier of the μ-th OFDM symbol, $\Delta f = 1/T_\mathrm{OFDM}$ is the subcarrier spacing, T_OFDM is the OFDM symbol duration, T_CP is the cyclic prefix (CP) duration, $T_\mathrm{SRI} = T_\mathrm{OFDM} + T_\mathrm{CP}$ is the symbol repetition interval (SRI) and $t \in [\mu T_\mathrm{SRI}, (\mu+1) T_\mathrm{SRI})$.

The μ-th received OFDM symbol in baseband without CP in presence of noise and interference can be represented as

$$\begin{aligned} y_\mu(t) = &\sum_{p=1}^{N_\mathrm{targ}} a(p) x_\mu(t - \tau_\mu(p)) e^{-j2\pi f_c \tau_\mu(p)} + w_\mu(t) \\ &+ v_\mu(t), \quad t \in [\mu T_\mathrm{SRI} + T_\mathrm{CP}, (\mu+1) T_\mathrm{SRI}) \end{aligned} \tag{2}$$

978-0-9928-6265-7/16/$31.00 ©2016 IEEE

where N_{targ} is the number of targets, p is the target index, $a(p)$ is the amplitude and $\tau_\mu(p)$ is the round-trip delay of the μ-th OFDM symbol for p-th target, f_c is the carrier frequency, $w_\mu(t)$ is the noise and $v_\mu(t)$ is the interfering signal.

The signal model in (2) is based on two assumptions, both typical and realistic for OFDM radar: *a*) the signal attenuation for p-th target $a(p)$ is frequency-flat and time-invariant and *b*) the Doppler shift of subcarriers is negligible due to a suitable system parametrization. For simplicity, we further assume that *c*) $x_\mu(t-\tau_\mu(p)) = x_\mu(t-\tau_{\mu=0}(p))$, i.e. the range migration for the baseband signal $x_\mu(t)$ during one measurement cycle of N_{sym} OFDM symbols is negligible. This assumption is however not necessary for the interference suppression algorithm in Section III, since it treats each OFDM symbol individually.

Substituting $x_\mu(t)$ in (1) into (2) and sampling at Nyquist rate after the CP, i.e. at $t = mT_{\text{OFDM}}/N_\text{c} + T_{\text{CP}}$, $m \in [0, N_\text{c})$, the μ-th discrete-time OFDM symbol $y_\mu[m] \triangleq y_\mu(mT_{\text{OFDM}}/N_\text{c} + T_{\text{CP}})$ can be written as

$$\begin{aligned} y_\mu[m] =& \frac{1}{N_\text{c}} \sum_{n'=0}^{N_\text{c}-1} s_\mu(n') e^{j2\pi \frac{n'm}{N_\text{c}}} \sum_{p=1}^{N_{\text{targ}}} e^{-j2\pi n \Delta f \tau_0(p)} \\ & \cdot a(p) q_\mu(p) + w_\mu[m] + v_\mu[m], \ n' \in [0, N_\text{c}) \end{aligned} \tag{3}$$

where $q_\mu(p) = e^{-j2\pi f_\text{c} \tau_\mu(p)}$ is the carrier-induced phase shift of the μ-th OFDM symbol due to the delay $\tau_\mu(p)$, used later for velocity estimation. An FFT is performed over each OFDM symbol to obtain the spectrum $Y_\mu(n)$ with orthogonal subcarriers:

$$\begin{aligned} Y_\mu(n) =& \sum_{m=0}^{N_\text{c}-1} y_\mu[m] e^{-j2\pi \frac{nm}{N_\text{c}}} = s_\mu(n) \sum_{p=1}^{N_{\text{targ}}} a(p) q_\mu(p) \\ & \cdot e^{-j2\pi n \Delta f \tau_0(p)} + W_\mu(n) + V_\mu(n), \quad n \in [0, N_\text{c}) \end{aligned} \tag{4}$$

where $W_\mu(n)$ and $V_\mu(n)$ are the FFT of $w_\mu[m]$ and $v_\mu[m]$, respectively. Note that (4) holds due to

$$\begin{aligned} \sum_{n'=0}^{N_\text{c}-1} s_\mu(n') \sum_{m=0}^{N_\text{c}-1} e^{j2\pi \frac{(n'-n)m}{N_\text{c}}} &= \sum_{n'=0}^{N_\text{c}-1} s_\mu(n') \delta(n'-n) = \\ &= N_\text{c} s_\mu(n), \quad n \in [0, N_\text{c}) \end{aligned} \tag{5}$$

where $\delta(n'-n)$ is the Kronecker delta function defined as:

$$\delta(n'-n) = \begin{cases} 1, & n = n' \\ 0, & n \neq n' \end{cases}. \tag{6}$$

To eliminate the transmitted complex modulation symbols $s_\mu(n)$, a spectral division is carried out:

$$\begin{aligned} Z_\mu(n) =& \frac{Y_\mu(n)}{s_\mu(n)} = \sum_{p=1}^{N_{\text{targ}}} a(p) q_\mu(p) e^{-j2\pi n \Delta f \tau_0(p)} \\ & + \frac{W_\mu(n)}{s_\mu(n)} + \frac{V_\mu(n)}{s_\mu(n)}. \end{aligned} \tag{7}$$

As it can be seen from (7), the noise and interference are not amplified through the complex division if the modulation symbols $s_\mu(n)$ have unit amplitudes and varying phases over n. In this case, both the noise and interference are influenced only in phase by the spectral division. In case the radar signal s_μ and the interference V_μ are not correlated, the spectral division leads to a decorrelation of the interference $V_\mu(n)$ over n and thus in distance, and if $s_\mu(n)$ is changing over μ, also in slow-time μ and thus in velocity.

$Z_\mu(n)$ contains a sum of complex sinusoids whose frequencies correspond to the round-trip-delays, i.e. to the distances to the targets. Thus, to create the distance profile of the μ-th OFDM symbol, an IFFT is performed on $Z_\mu(n)$:

$$\begin{aligned} z_\mu(k) =& \frac{1}{N_\text{c}} \sum_{n=0}^{N_\text{c}-1} Z_\mu(n) e^{j2\pi \frac{nk}{N_\text{c}}} = \frac{1}{N_\text{c}} \sum_{p=1}^{N_{\text{targ}}} a(p) q_\mu(p) \\ & \cdot u_\text{d}(k,p) + (w_\mu \star x_\mu^*)[k] + (v_\mu \star x_\mu^*)[k], \ k \in [0, N_\text{c}) \end{aligned} \tag{8}$$

where $u_\text{d}(k,p) = \sum_{n=0}^{N_\text{c}-1} e^{-j2\pi \frac{n}{N_\text{c}}(N_\text{c}\Delta f \tau_0(p) - k)}$ denotes the integration gain of the p-th target in the k-th distance bin, "$\star$" denotes the circular discrete correlation and "*" denotes the complex conjugate. The latter holds because for unit amplitude modulation symbols $s_\mu(n)$, $(W_\mu(n) + V_\mu(n))/s_\mu(n) = (W_\mu(n) + V_\mu(n)) s_\mu^*(n)$. Finally, an FFT is performed over OFDM symbols. The result for the k-th distance bin is:

$$\begin{aligned} Q_k(l) =& \frac{1}{N_\text{c}} \sum_{\mu=0}^{N_{\text{sym}}-1} z_k(\mu) e^{-j2\pi \frac{\mu l}{N_{\text{sym}}}} = \frac{1}{N_\text{c}} \sum_{p=1}^{N_{\text{targ}}} a(p) \\ & \cdot u_\text{v}(l,p) u_\text{d}(k,p) + Q_{\text{w}_k}(l) + Q_{\text{v}_k}(l), \quad l \in [0, N_{\text{sym}}) \end{aligned} \tag{9}$$

where $u_\text{v}(l,p) = \sum_{\mu=0}^{N_{\text{sym}}-1} e^{-j2\pi \left(f_\text{c} \tau(\mu,p) + \frac{\mu l}{N_{sym}} \right)}$ is the integration gain in the velocity dimension, $Q_{\text{w}_k}(l)$ and $Q_{\text{v}_k}(l)$ are the FFTs of the noise and interference terms in (8), l is the velocity bin index. As (7) - (9) show, the interfering signal is decorrelated in both distance and velocity through the OFDM processing steps, whereas the desired signal is compressed into one (d,v) bin. This prevents the occurrence of ghost targets due high interference peaks and enables a high SIR and dynamic range as shown in Section IV.

III. Interference Suppression Algorithm

In this section we present an interference suppression method for OFDM radar for arbitrary narrowband interferences. An interference is considered as narrowband if its occupied bandwidth during one OFDM symbol is much smaller than that of the OFDM radar. This is the case for an FMCW radar with the same bandwidth as the OFDM radar, but with frequency ramps of a much longer duration than an OFDM symbol. In this case, the interference affects only a small band of contiguous OFDM subcarriers. This property is used for the interference suppression method presented in this section.

The proposed interference suppression algorithm operates on each OFDM symbol $\underline{Z}_\mu = [Z_\mu(0), .., Z_\mu(N_\text{c}-1)]^T$ in (7). With this in mind, the index "μ" will be omitted in the following. The interference suppression is achieved in three steps: interference detection, least-squares estimation of prediction coefficients from unaffected subcarriers and FBLP of the samples affected by interference.

In case of a considerable interference power, the subcarriers occupied by an interfering signal will have a much higher amplitude than the unaffected ones. Thus, these subcarriers can be detected based on their amplitude, e.g. with a constant false-alarm rate (CFAR) detector. They will be then excluded from processing to drop the major part of the interference.

However, the exclusion of affected samples from processing by replacement of their values with zeros leads to gaps in frequency samples, which will lead to increased sidelobes after the IFFT in (8). This might limit the dynamic range in presence of targets with very high signal-to-noise ratio (SNR). To avoid this limitation, the values of affected subcarriers are recovered from neighbouring unaffected subcarriers via linear prediction.

Let us denote the index of the first and the last subcarrier in the band occupied by the detected interference with n_f and n_l respectively. It is well known that signals consisting of a sum of complex sinusoids such as the desired signal in $\underline{Z}$ in (7) have a linear dependency between the samples, which can be represented by an autoregressive (AR) model [10], [11]. In presence of noise, the set of linear equations describing this dependency can be represented in a matrix form as

$$\underbrace{\begin{bmatrix} Z(o-1) & \dots & Z(0) \\ \vdots & \ddots & \vdots \\ Z(n_\mathrm{f}-2) & \dots & Z(n_\mathrm{f}-o-1) \\ Z(n_\mathrm{l}+o) & \dots & Z(n_\mathrm{l}+1) \\ \vdots & \ddots & \vdots \\ Z(N_\mathrm{c}-2) & \dots & Z(N_\mathrm{c}-o-1) \end{bmatrix}}_{\mathbf{B}} \cdot \underbrace{\begin{bmatrix} g_\mathrm{fp}(1) \\ g_\mathrm{fp}(2) \\ \vdots \\ g_\mathrm{fp}(o) \end{bmatrix}}_{\underline{g}_\mathrm{fp}} \approx \underbrace{\begin{bmatrix} Z(o) \\ \vdots \\ Z(n_\mathrm{f}-1) \\ Z(n_\mathrm{l}+o+1) \\ \vdots \\ Z(N_\mathrm{c}-1) \end{bmatrix}}_{\underline{b}} \tag{10}$$

where $o > N_\mathrm{targ}$ is the assumed order of the system and $\underline{g}_\mathrm{fp}$ is the vector of forward linear prediction (FP) coefficients. The model order o has to be higher than the maximum number of targets expected. However, o defines the minimum number of adjacent subcarriers necessary for prediction, thus, should not be unnecessarily large. For details on the choice of the system order o please refer to [11].

A least squares estimate of $\underline{g}_\mathrm{fp}$ is given by

$$\underline{g}_\mathrm{fp} = (\mathbf{B}^\mathrm{H}\mathbf{B})^{-1}\mathbf{B}^\mathrm{H}\underline{b}. \tag{11}$$

where the superscript "H" denotes the conjugate transpose. In linear prediction notation (11) can be rewritten as

$$\underline{g}_\mathrm{fp} = \mathbf{R}^{-1}\underline{r} \tag{12}$$

where $\mathbf{R} = \mathbf{B}^\mathrm{H}\mathbf{B}$ is the correlation matrix and $\underline{r} = \mathbf{B}^\mathrm{H}\underline{b}$ is the correlation vector obtained from the measurement data. Alternatively, the autocorrelation function of $\underline{Z}_\mu$ is estimated and $\underline{g}_\mathrm{fb}$ is calculated by the Levinson-Durbin algorithm [12], [13] which is computationally more efficient than the LS estimate in (12).

According to the theory of optimum linear prediction [11], the backward prediction (BP) coefficients $\underline{g}_\mathrm{bp}$ can be obtained from $\underline{g}_\mathrm{fp}$ with

$$\underline{g}_\mathrm{bp} = \mathbf{T}\,\underline{g}^*_\mathrm{fp}, \quad \mathbf{T} = \begin{bmatrix} 0 & \cdots & 1 \\ & \iddots & \\ 1 & \cdots & 0 \end{bmatrix} \tag{13}$$

where $\mathbf{T}$ is the permutation matrix that swaps the coefficients of $\underline{g}_\mathrm{fp}$. Consecutively, the missing samples of all affected subcarriers are predicted recursively in forward and backward directions:

$$Z_\mathrm{fp}(i_\mathrm{fp}) = [Z(i_\mathrm{fp}-1), \dots, Z(i_\mathrm{fp}-o)] \cdot \underline{g}_\mathrm{fp} \tag{14}$$

$$Z_\mathrm{bp}(i_\mathrm{bp}) = [Z(i_\mathrm{bp}+o), \dots, Z(i_\mathrm{bp}+1)] \cdot \underline{g}_\mathrm{bp} \tag{15}$$

with $i_\mathrm{fp} = (n_\mathrm{f}, n_\mathrm{f}+1, \dots, n_\mathrm{l})$ and $i_\mathrm{bp} = (n_\mathrm{l}, n_\mathrm{l}-1, \dots, n_\mathrm{f})$. Both predictions can be further averaged to obtain a better estimate for the missing samples:

$$Z(n_\mathrm{i}) = \frac{(Z_\mathrm{fp}(n_\mathrm{i}) + Z_\mathrm{bp}(n_\mathrm{i}))}{2}, \quad n_f \le n_i \le n_l \tag{16}$$

Then, the further OFDM processing steps described in Section II can be performed.

Even though described for a single band affected by interference, the presented approach can be analogously applied if multiple narrow bands are affected.

IV. Results

In this section the performance of the proposed algorithm is studied with simulations and measurements. Both measurements and simulations are done with OFDM subcarriers modulated with complex modulation symbols of unit amplitudes and random phases. A Kaiser window with $\beta = 7.7$ is used for sidelobe suppression for FFTs in (8) and (9). For the interference suppression, the model order is set to $o = 50$.

A. Simulations

An OFDM radar interfered by an FMCW radar at $77\,\mathrm{GHz}$ is simulated. Both systems have the same bandwidth of $B = 625\,\mathrm{MHz}$. For the OFDM radar this bandwidth is shared between $N_\mathrm{c} = 1024$ OFDM subcarriers. Chirp duration is $T_{ch} = 5\,\mathrm{ms}$, whereas with $T_{SRI} = 12.29\,\mu\mathrm{s}$ and $N_\mathrm{sym} = 512$ a duration of measurement cycle of $T_\mathrm{cycle} = 6.3\,\mathrm{ms}$ is achieved for the OFDM radar. Both FMCW and OFDM signals have the same power at the receiver input.

This configuration results in detection of 3 to 5 subcarriers affected by the interference for each OFDM symbol. For the detection of those subcarriers a CFAR detector is used.

A target at the distance $d = 25\,\mathrm{m}$ and velocity of $v = -10\,\mathrm{m/s}$ is simulated in a noiseless setup. The OFDM signal overlapped by the interfering chirp is shown in Fig. 1 (a). The result obtained after (d,v) processing without interference suppression is shown in Fig. 1 (b). A mean SIR of $51.3\,\mathrm{dB}$ is achieved, which corresponds to the integration gain of 2D FFT. In Fig. 1 (c), the (d,v) image with interference suppression is shown. A mean SIR of $64.25\,\mathrm{dB}$ is obtained, which corresponds to a $13\,\mathrm{dB}$ SIR improvement.

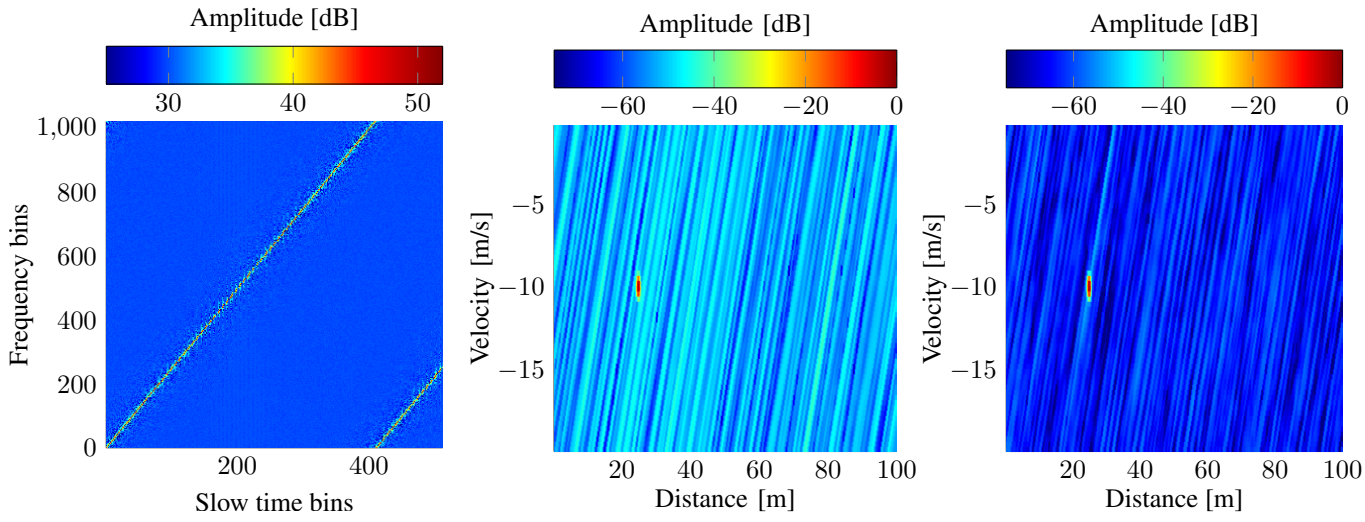

Fig. 1: OFDM radar distance-velocity estimation in presence of interference: (a) OFDM signal overlapped with interference, (b) (d,v) image without interference suppression, (c) (d,v) image with interference suppression.

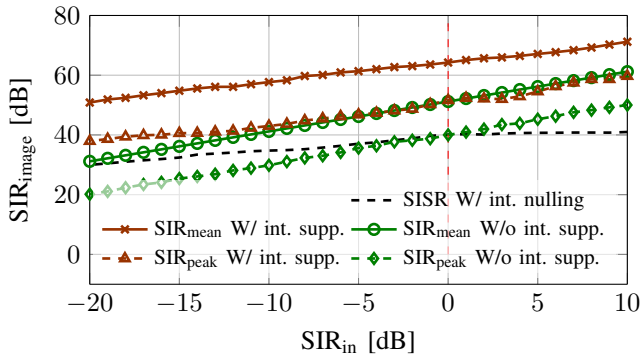

Fig. 2: SIR in (d,v) estimation over the input SIR

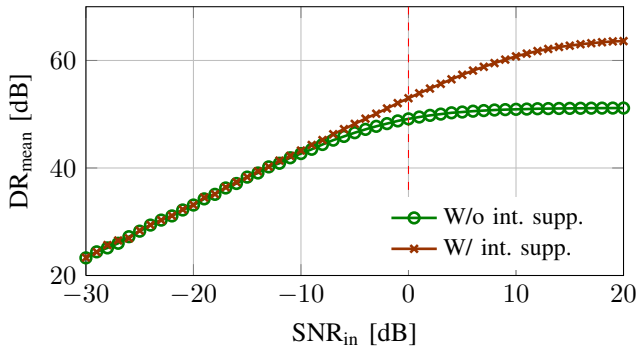

Fig. 3: Mean dynamic range in (d,v) estimation over the input SNR for $\mathrm{SIR}_{\mathrm{in}} = 0$

For quantitative performance evaluation of the presented algorithm, the dependency of the mean SIR in (d,v) space as well as the SIR with respect to the highest interference peak is shown in Fig. 2. Furthermore, to demonstrate the need for a recovery of the samples affected by interference, the signal-to-interference-and-sidelobe-ratio (SISR) in case of just nulling the affected samples is shown. As it can be seen, the replacement the affected subcarriers' values with zeros leads to increase of sidelobes, which, depending on SNR, might

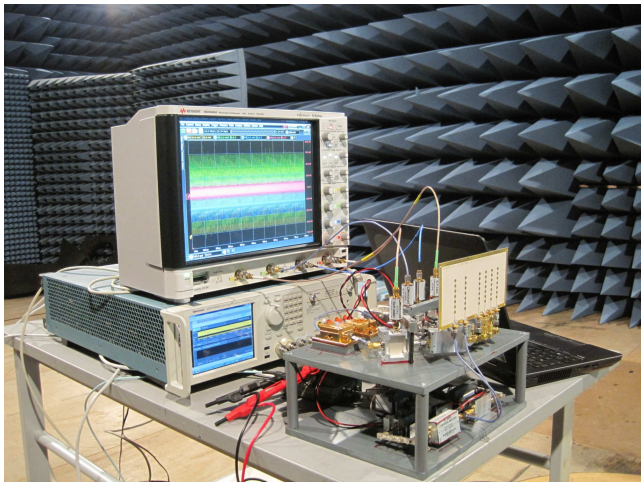

Fig. 4: OFDM-MIMO radar setup used for measurements

limit the dynamic range. Thus, a recovery of nulled samples is necessary, especially in case targets with a high SNR are present. Clearly, with the proposed method the SIR achieved through (d,v) processing can further be increased by 12–16 dB.

To demonstrate the performance of the proposed algorithm in presence of noise, the mean dynamic range ($\mathrm{DR}_{\mathrm{mean}}$) over SNR for $\mathrm{SIR} = 0\,\mathrm{dB}$ is presented in Fig. 3. The term mean dynamic range refers to the ratio of the highest peak power to the mean power of noise, interference and sidelobes. As it can be seen, in case of a low SNR, i.e. when the noise is more significant than the interference ($\mathrm{SNR}_{\mathrm{in}} < -15\,\mathrm{dB}$), the DR is limited by the noise. Starting from $-15\,\mathrm{dB}$, the interference has a visible effect on the DR, and the proposed algorithm is able to achieve an improvement. For $\mathrm{SNR}_{\mathrm{in}} > -7\,\mathrm{dB}$, without interference suppression the dynamic range is limited almost completely by the interference and no significant DR improvement over increasing SNR is obtained. In this region the proposed algorithm achieves an increase of the DR via

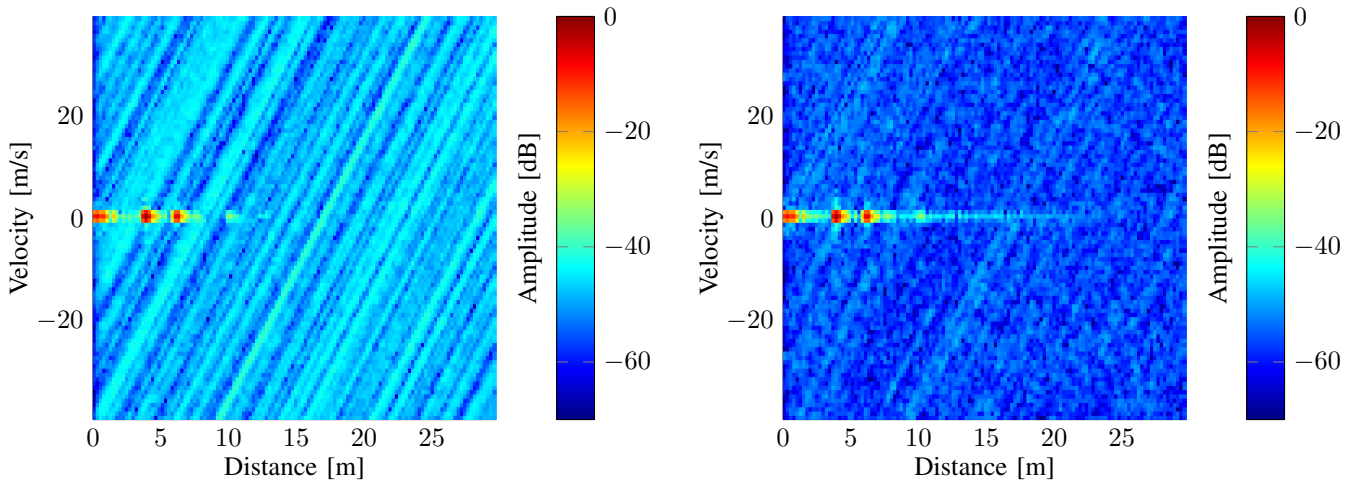

Fig. 5: (a): measured (d,v) image without interference suppression, (b): measured (d,v) image with improved SIR through interference suppression

interference suppression, which tends asymptotically to the interference suppression in the noiseless case for $\mathrm{SNR}_{\mathrm{in}} > 5\,\mathrm{dB}$.

B. Measurements

To verify the results presented in Section IV-A, measurements with a prototype OFDM radar at $24.5\,\mathrm{GHz}$ have been taken in an anechoic chamber. One of two transmitters of the multiple-input-multiple-output OFDM radar is programmed to transmit an FMCW signal and represents an interferer for the other transmit antenna operating as OFDM radar transmitter (Fig. 5). Due to the direct coupling between antennas the interference has a higher input power than the OFDM radar signal. All radar parameters except the carrier frequency are as in Section IV-A. Two stationary targets (corner reflectors) at the distance of $4.7\,\mathrm{m}$ and $6.4\,\mathrm{m}$ are present.

A mean SIR of $\approx 48\,\mathrm{dB}$ and a peak SIR of $38.7\,\mathrm{dB}$ has been achieved in measurements. Through interference suppression an increased mean SIR of $\approx 58.8\,\mathrm{dB}$ and a peak SIR of $48.96\,\mathrm{dB}$ have been obtained. After interference suppression the interference level is comparable with the noise floor.

Furthermore, the measurements show the robustness of the presented method against multipath propagation of interference, since the interfering signal arrives at the receiver through multiple paths: over the direct coupling and via reflection from targets.

V. Conclusion

In this paper we discussed the issue of interference for OFDM radar and described the effect of OFDM signal processing steps on the interfering signal. We have shown that the interference is decorrelated in (d,v) space through the processing steps, which already leads to a high SIR. We also presented a method for suppression of narrowband interference and demonstrated its performance in example of an FMCW interferer with slow ramps. Whereas for chosen parameters a mean SIR of $51\,\mathrm{dB}$ has been achieved in simulations, a further SIR improvement of 12–$16\,\mathrm{dB}$ has been obtained by the proposed interference suppression algorithm. Finally, measurements with a prototype OFDM radar have validated the results.

References

[1] N. Levanon, "Multifrequency complementary phase-coded radar signal." in *IEEE Proceedings on Radar, Sonar and Navigation*, 2000.

[2] D. Garmatyuk, J. Schuerger, Y. Morton, K. Binns, M. Durbin, and J. Kimani, "Feasibility study of a multi-carrier dual-use imaging radar and communication system," in *Radar Conference, 2007. EuRAD 2007*, 2007, pp. 194–197.

[3] R. Tigrek, W. de Heij, and P. van Genderen, "Solving Doppler ambiguity by Doppler sensitive pulse compression using multi-carrier waveform," in *Radar Conference, 2008. EuRAD 2008*, 2008, pp. 72–75.

[4] C. Sturm, T. Zwick, and W. Wiesbeck, "An OFDM system concept for joint radar and communications operations," in *Vehicular Technology Conference, 2009. VTC Spring 2009. IEEE*, 2009, pp. 1–5.

[5] X.-G. Xia, T. Zhang, and L. Kong, "MIMO OFDM radar IRCI free range reconstruction with sufficient cyclic prefix," *Aerospace and Electronic Systems, IEEE Transactions on*, vol. 51, no. 3, pp. 2276–2293, July 2015.

[6] T. Zhang, X.-G. Xia, and L. Kong, "IRCI free range reconstruction for SAR imaging with arbitrary length OFDM pulse," *IEEE Transactions on Signal Processing*, vol. 62, no. 18, pp. 4748–4759, 2014.

[7] T. Zhang and X.-G. Xia, "OFDM synthetic aperture radar imaging with sufficient cyclic prefix," *IEEE Transactions on Geoscience and Remote Sensing*, vol. 53, no. 1, pp. 394–404, 2015.

[8] C. Sturm, Y. Sit, M. Braun, and T. Zwick, "Spectrally interleaved multi-carrier signals for radar network applications and multi-input multi-output radar," *Radar, Sonar & Navigation, IET*, vol. 7, no. 3, pp. 261–269, March 2013.

[9] Y. L. Sit and T. Zwick, "MIMO OFDM radar networks: Inter- & intra-system interference handling," *Asia-Pacific Microwave Conference (APMC)*, no. 1318-1320, 2014.

[10] D. W. Tufts and R. Kumaresan, "Estimation of frequencies of multiple sinusoids: Making linear prediction perform like maximum likelihood," *Proceedings of the IEEE*, vol. 70, no. 9, pp. 975–989, Sept. 1982.

[11] S. Haykin, *Adaptive Filter Theory, 5th edition*, A. Gilfillan, Ed. Pearson, 2014.

[12] N. Levinson, "The Wiener RMS (root mean square) error criterion in filter design and prediction," *J. Math. Phys.*, vol. 25, no. 4, pp. 261–278, 1947.

[13] J. Durbin, "Efficient estimation of parameters in moving-average models," *Biometrika*, vol. 46, p. 306316, 1959.